Supplemental

Methods

ALS sample

Penn UMN score

The Penn UMN score ranged from 0 to 32 points and comprised items from the bulbar segment (0-4 points) and from each of the four limbs (0-7 points per limb) [1]. In detail, for the bulbar segment, single points were allocated for an abnormal jaw-jerk reflex, an abnormal facial reflex, the existence of the palmomental sign and the existence of an abnormal pseudobulbar affect. For the upper extremity subscore, single points were given for each, pathologically brisk biceps reflex, triceps reflex, presence of finger flexors, Hoffmann's sign or the existence of a clonus anywhere in the limb. Additionally, spasticity was rated according to the Ashworth Spasticity Scale (0-2 points, with adding 0 points for Ashworth 1 (normal tone), 1 point for Ashworth 2-3, 2 points for Ashworth 4-5) [2]. For the lower extremity subscore, single points were allocated for each, pathologically brisk plantar reflex, ancle reflex, crossed adduction, Babinski's sign and a clonus anywhere in the limb. For the lower extremity, spasticity was rated the same way as described for the upper extremity subscore.

Clinical phenotypes

Clinical phenotypes were classified according to recent specifications [3, 4]. At the time of study inclusion, a variable combination of UMN signs (spastic tone, clonus, etc.) and LMN signs (wasting, weakness, fasciculations) in the upper and lower limbs were found in those designated as classic ALS who, in turn, fulfilled the El Escorial criteria of definite or probable ALS. UMND ALS patients had either no LMN signs, or, if present (1) they were restricted to only 1 neuraxis level (bulbar, cervical, or lumbosacral); and (2) electromyographic abnormalities were limited to sparse fibrillation potentials/positive sharp waves or minor enlargement of motor unit potentials in 1 or at most 2 muscles [5, 6] for at least 12 months after symptom onset. The diagnostic criteria for PLS required a period of at least 4 years in

which there were only UMN signs on examination. Other conditions that mimic PLS, such as hereditary spastic paraplegia (HSP) were excluded by appropriate investigations [7]. All patients with LMND ALS had clinical and electrophysiological evidence of sporadic progressive pure LMN involvement in 1 or more regions without clinical signs of UMN dysfunction. To differentiate this condition from early limb-onset ALS, we specified that LMN involvement must be the predominant finding for at least 12 months after the symptom onset. LMND ALS comprised patients with flail arm phenotype (n=4), flail leg phenotype (n=2) and progressive muscular atrophy (n=3). Other LMN diseases, such as multifocal motor neuropathy, spinal muscular atrophy, monomelic amyotrophy, Kennedy's disease, and post-polio syndrome, were excluded by extensive clinical and laboratory examinations [7, 8].

Data availability

CSF data were on hand for all ALS patients, of those 89 cases, 58 (69%) and 13 (15%) patients, respectively, have already been included in our previous cross-sectional and longitudinal peripheral nerve sonography ALS studies [3, 9, 10]. Out of the 84 patients with available baseline ALSFRS-R scores, longitudinal ALSFRS-R scoring was performed in n=71 cases (80%) with at least two follow-ups and n=46 cases (52%) with at least three follow-ups. Survival data could be identified in n=86 subjects (97%) with n=53 (62%) having died after a median survival time of 35.8 months. C9orf72 and SOD1 status was available in n=64 patients (72%), comprising n=6 (9%) suffering from familial ALS (n=2 with C9orf72 positivity and n=4 with SOD1 positivity). Nerve CSA was available in n=72 (81%) cases, CMAP amplitudes in n=65 (73%) and MPRAGE images in n=61 (69%) subjects of whom n=51 (57%) had also cerebral DTI measures. Constellations of individual data availability in ALS are indicated in **Supplemental Figure 1.**

CSF measures

Within 20 minutes of lumbar puncture, CSF samples were centrifuged at 4 °C, aliquoted and stored at -80 °C until analysis. CSF biomarkers were measured with commercially available ELISA (for NfL: NF-light® ELISA, IBL International GmbH, Hamburg, Germany; for total tau

[ttau] or ptau: Innotest hTauAg or Innotest p-Tau, Innogenetics, Ghent, Belgium), following the instructions provided by the manufacturer.

To assess the performance of the NfL assay we determined the intra-assay coefficient of variability (CV; =reproducibility, within-assay performance) and the inter-assay CV (=repeatability, between-assay performance) [11]. CV was calculated using the root mean square method, described e.g. in [19]. CSF samples of 2 controls and four ALS patients were measured twice on the first assay, and procedure was repeated 24 hours later taking a second assay. Intra-assay CV of duplicates was 3.1%, inter-assay CV was 10.6%, which is in line with the literature [11]. Detailed CSF NfL values of each sample are given in **Supplemental Table 1**.

3T MRI measures of the brain

All MRI scans were performed on the same Siemens Verio 3 T system (Siemens Medical Systems, Erlangen, Germany) with a 32-channel head coil. 3D MPRAGE images were acquired using the following parameters: acquisition time 9 min, 20 s, repetition time 2500 ms, echo time 4.82 ms, inversion time 1100 ms, flip angle 7 °, voxel size = 1×1×1 mm^3. DWI data were acquired with a resolution of 2×2×2 mm^3. Diffusion gradients were applied along 30 non-collinear directions with b = 1000 s/mm^2, one scan without diffusion weighting (b = 0 s/mm^2) was also acquired. The data were averaged across two repetitions (for full details see [12, 13]). A T2-weighted FLASH sequence was acquired during the same session to investigate the presence of white matter hyperintensities.

Diffusion tensor imaging analysis

Diffusion tensor images were processed using the FMRIB software library (FSL [14]; Analysis Group, FMRIB, University of Oxford, UK). In brief, each diffusion weighted volume was affined-aligned to its corresponding b0 image using FSL's linear image co-registration tool (FLIRT v5.4.2) to correct for motion artifacts and eddy-current distortions. Using FSL's brain-extraction tool (BET v2.1) a binary brain mask of each b0 image was generated, with fractional threshold f = 0.1 and vertical gradient g = 0. The original b-matrix was reoriented

using an in-house script to adjust it for rotations induced by the previous transformations. FSL's diffusion toolbox (FDT v2.0) was used to fit a single tensor model, taking a weighted linear approach, and to compute the maps of DTI scalars (FA, mean diffusivity (MD), radial diffusivity (RD), axial diffusivity (AD)). Load of white matter lesion was evaluated on a T2-weighted FLASH sequence employing the Fazekas scale [15].

The analyses were performed employing tract-based spatial statistics [16] that warped all the FA images to the FMRIB58_FA standard template (FMRIB; resolution: 1×1×1 mm^3) in MNI152 space using FSL's non-linear registration tool (FNIRT v1.0). The warped FA maps were averaged to create a mean FA template, from which the FA skeleton was computed, imposing an FA threshold of 0.2. All the FA maps as well as the maps of the other DTI scalars were then projected onto the skeleton. The whole-brain regression analysis was conducted employing the Randomise tool version 2.9 available in FSL with 5000 permutations, threshold-free cluster enhancement (TFCE) and 2D optimization for tract-based DTI analysis. The CST region of interest (ROI) analysis was performed using the CST mask (bilateral) included in the JHU white matter tractography atlas available in FSL, thresholded at 0.5. The JHU-CST mask was further intersected with the study- specific skeleton and the resulting mask was used for extracting the median values of DTI scalars in the CST for each participant.

Cortical thickness and volumetric measures

For each patient cortical thickness of the bilateral precentral gyrus was obtained from the native-space MPRAGE scans using the automated FreeSurfer 6.0 parcellation [18]. Total brain volume (TBV), GM volume (GMV) and WM volume (WMV), normalized for head size, were estimated using the SIENAX algorithm from the SIENA-package of FSL v5.0.

Results

Relationship between CSF NfL and DTI metrics across ALS phenotypes

Out of the whole sample n=29 classic ALS, n=14 LMND ALS and n=6 UMND ALS cases had available both, measures of CSF NfL and DTI metrics. Unfortunately, in our cohort the group of LMND ALS and UMND ALS was too small, lacking the power to perform phenotype-wise analysis. However, correlation between DTI metrics in the CST and NfL level was present also when restricting the analysis to the classic ALS cases (NfL and FA: rho=-0.4, p=0.03; NfL and RD: rho=0.4, p=0.05; **Supplemental Figure 2**). Results in classic ALS are convincing, overall supporting our main findings of a significant relationship between CSF NfL and CST integrity.

Relationship between CSF NfL and survival across ALS phenotypes

The distribution of observed survival times over measured NfL levels is shown in **Supplemental Figure 3A** for the distinct phenotypes. Classic phenotypes with survival times greater than 8 years were excluded as they seem to exhibit a somewhat different course of disease. Within that plot, the distribution of the values of the UMND ALS phenotype is seemingly different from that of the scatter pattern of the classic phenotype. To elucidate this, a principal component analysis with the variables NfL and survival time was performed yielding the eigenvectors shown as arrows in black. The factor loads of [-0.7, 0.7] and [0.7, 0.7] lead to factor 1 describing constellations with low NfL values and comparatively longer survival times and factor 2 pointing to individuals with longer survival times despite higher NfL values. The scatter plot in factor coordinates in **Supplemental Figure 3B** reveals that patients with the classic phenotype tend to scatter along the factor 1 axis, displaying low NfL and relatively long survival times or for negative factor 1 values a combination of high NfL with short survival times. The UMND group displays a negative mean for factor 1, so that they also seem to exhibit elevated NfL levels corresponding to decreased survival times. But this is somewhat offset by a positive mean value in their factor 2 components, allowing for constellations with higher NfL levels than comparably long-lived classic cases or the ability to survive longer than would be expected for a classic case with these NfL levels (or a combination of those two). One may thus hypothesize that these results point to the

existence of distinct groups displaying high CSF NfL: UMND ALS with longer survival despite high CSF NfL and ALS patients with combined UMN and LMN pathology (classic disease phenotype), high CSF NfL and worse prognosis.

Tables

Supplemental Table 1. Stability of the NfL assay

Repeated measurements (M) were carried out using two different assays (A1 at day 1 and A2 at day 2). Between-assay repeatability was 10.6%, and within-assay reproducibility was 3.1%. CSF NfL is given in pg/ml.

Subject code	A1M1	A1M2	A2M1	A2M2
372/18L	365	397	342	333
433/18L	365	373	343	342
404/17	12,092	12,551	10,175	10,232
613/17	50,000	50,000	39,875	36,536
191/18	10,671	11,247	10,788	11,061
347/18	2,020	2,052	1,885	1,973

Supplemental Table 2. Demographics, diagnoses, CSF NfL, ptau and ttau levels as well as the ptau/ttau ratio of disease controls

Subject code	Age (years)	Sex	Diagnosis	CSF NfL (pg/ml)	CSF ttau (pg/mgl)	CSF ptau (pg/ml)	ptau/ttau
305/14L	35	Female	Non-specific headache	612			
217/15L	39	Male	Non-specific headache	655			
866/16L	39	Female	Non-specific cognitive complaints	771	122	33	0.27
095/14L	41	Female	Fibromyalgia	832			
950/14L	44	Male	Non-specific pain	852			
229/14L	41	Male	Adie's tonic pupil	933			
298/14L	51	Female	Paresthesia	943			
754/14L	42	Male	Non-specific headache	972			
469/15L	62	Female	Radial bone fracture	982	293	59	0.20
843/14L	35	Female	Somatoform disorder	993			
021/16L	70	Female	Traumatic injury	1010	316	70	0.22
1280/14L	47	Female	Somatoform disorder	1029			
848/13L	60	Male	Chronic pain	1066		20	
037/14L	58	Female	Depression	1067	162		
922/14L	38	Female	Somatoform disorder	1091			
100/16L	64	Male	Shoulder pain	1160	139	28	0.20
1299/14L	69	Female	Cognitive complaints	1193	373	65	0.17
862/15L	68	Male	Shoulder pain	1233	308	63	0.20
341/16L	75	Female	Pain	1345	216	48	0.22
768/14L	37	Male	Non-specific headache	1387			
902/16L	74	Male	Pain	1415	163	37	0.23
387/14L	32	Female	Non-specific headache	1424			
280/10L	70	Female	Paresthesia	1439			
848/16L	66	Male	Chronic pain	1553	306	80	0.26
136/16L	62	Male	Non-specific headache	1556	323	57	0.18
679/14L	46	Female	Somatoform disorder	1569			
477/13L	63	Male	Dyspnea	1635			
044/16L	73	Female	Paresthesia	1807	260	59	0.23
306/13L	60	Male	Paresthesia	1882			
836/15L	75	Male	Depressive episode	1884	250	47	0.19
995/15L	76	Male	Traumatic injury	2010	200	41	0.21
534/15	65	Male	Pain	2593	284	53	0.19
263/10L	71	Female	Somatoform disorder	2616			

Supplemental Table 3. Demographics and clinical data of the clinical ALS phenotypes

	Classic ALS (n=46)	**LMND ALS (n=31)**	**UMND ALS (n=10)**	**P-value**
Age, in years	64 (35-83)	63 (33-83)	60 (40-79)	0.7*
Male sex, n (%)	25 (54)	19 (61)	9 (90)	0.09#
Sporadic ALS / Familial ALS, n (%)	36 (90) / 4 (10)	19 (95) / 1 (5)	6 (86) / 1 (14)	0.9#
Disease onset bulbar / limb, n (%)	24 (48) / 22 (52)	2 (7) / 29 (94)	3 (30) / 7 (70)	0.001#
Disease duration, in months	9 (0.3-126)	15 (4-190)	11 (0.2-35)	0.1*
Disease progression rate, in 1 / months	0.8 (0.05-2.4)	0.4 (0.08-3.3)	0.7 (0.04-3.2)	0.2*
ALSFRS-R total score / 48, baseline	42 (22-48)	41 (20-46)	41 (28-46)	0.4*

Unless otherwise reported, medians and (ranges) are given. ALS, amyotrophic lateral sclerosis; ALSFRS-R, revised ALS functional rating scale; LMND, lower motor neuron dominant; UMND, upper motor neuron dominant; *ANOVA, #binary logistic regression analysis. P-values <0.05 were deemed to be statistically significant.

Figures

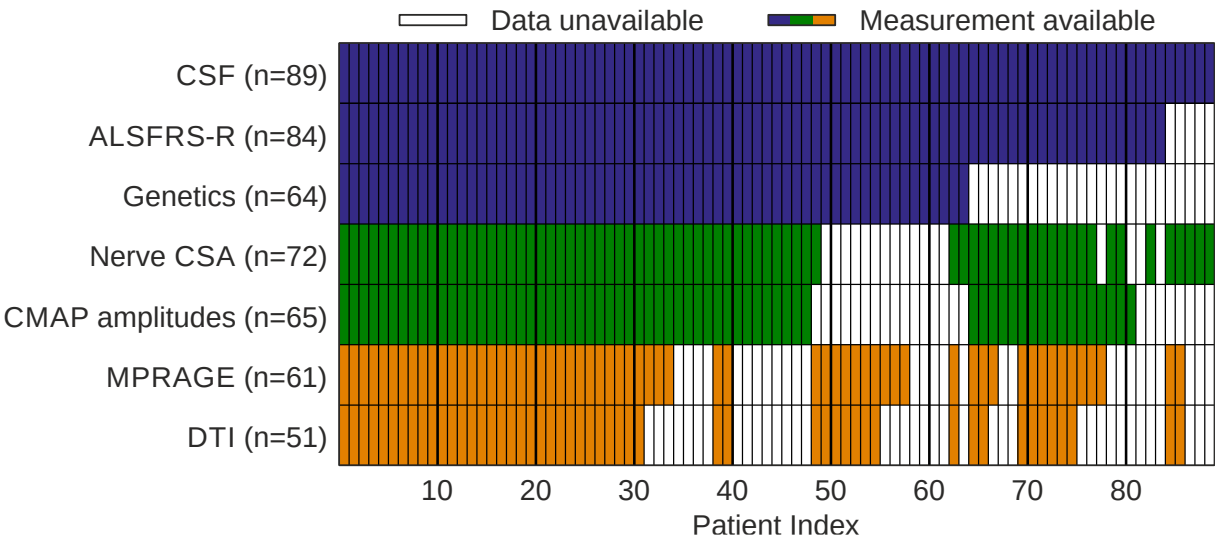

Supplemental Figure 1. Availability of multimodal data in the ALS sample

Constellations of data availability for the various measurements within the ALS sample. CSF, clinical and genetic measures are colored in blue, measures to obtain PNS neuroaxonal injury are colored in green and measures to obtain CNS neuroaxonal injury are colored in orange.

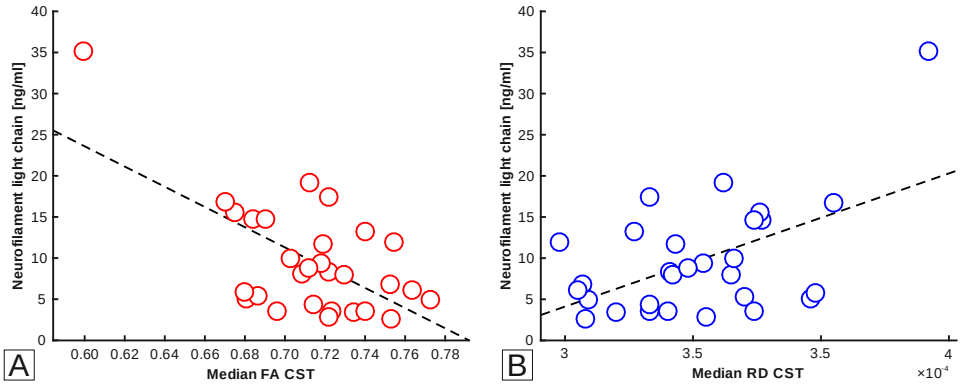

Supplemental Figure 2. Relationship between the DTI metrics and CSF NfL in patients with classic ALS phenotype

For the patient subgroup with classic ALS phenotype, the relationship depicted between CSF NfL and median FA or RD of the CST using a ROI-based approach is demonstrated in **A&B**.

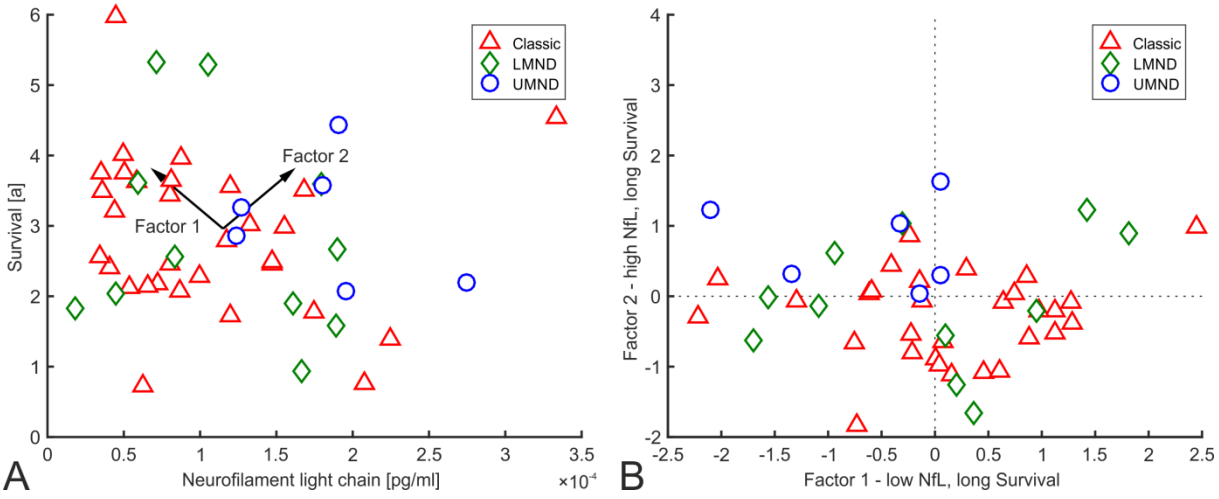

Supplemental Figure 3. Scatter plot of observed survival times vs. NfL measurement

The distribution of observed survival times over measured NfL levels is shown in **A** for the distinct ALS phenotypes. A principal component analysis was performed using the NfL levels and the survival times. The scatter plot in factor coordinates is displayed in **B.**

References

1. Woo JH, Wang S, Melhem ER et al. (2014) Linear associations between clinically assessed upper motor neuron disease and diffusion tensor imaging metrics in amyotrophic lateral sclerosis. PLoS. One. 9(8): e105753. doi: 10.1371/journal.pone.0105753
2. Bohannon RW, Smith MB (1987) Interrater reliability of a modified Ashworth scale of muscle spasticity. Phys Ther 67(2): 206–207
3. Schreiber S, Abdulla S, Debska-Vielhaber G et al. (2015) Peripheral nerve ultrasound in amyotrophic lateral sclerosis phenotypes. Muscle Nerve 51(5): 669–675
4. Chio A, Calvo A, Moglia C et al. (2011) Phenotypic heterogeneity of amyotrophic lateral sclerosis: a population based study. J. Neurol. Neurosurg. Psychiatry 82(7): 740–746
5. Soraru G, Ermani M, Logroscino G et al. (2010) Natural history of upper motor neuron-dominant ALS. Amyotroph. Lateral. Scler. 11(5): 424–429
6. Gordon PH, Cheng B, Katz IB et al. (2009) Clinical features that distinguish PLS, upper motor neuron-dominant ALS, and typical ALS. Neurology 72(22): 1948–1952
7. Gordon PH, Cheng B, Katz IB et al. (2006) The natural history of primary lateral sclerosis. Neurology 66(5): 647–653
8. van den RM B-V, van den Berg LH, Visser J et al. (2003) The spectrum of lower motor neuron syndromes. J. Neurol. 250(11): 1279–1292
9. Schreiber S, Debska-Vielhaber G, Abdulla S et al. (2018) Peripheral nerve atrophy together with higher cerebrospinal fluid progranulin indicate axonal damage in amyotrophic lateral sclerosis. Muscle Nerve 57(2): 273–278. doi: 10.1002/mus.25682
10. Schreiber S, Dannhardt-Stieger V, Henkel D et al. (2016) Quantifying disease progression in amyotrophic lateral sclerosis using peripheral nerve sonography. Muscle Nerve 54(3): 391–397
11. Koel-Simmelink MJA, Vennegoor A, Killestein J et al. (2014) The impact of pre-analytical variables on the stability of neurofilament proteins in CSF, determined by a novel validated SinglePlex Luminex assay and ELISA. J Immunol Methods 402(1-2): 43–49. doi: 10.1016/j.jim.2013.11.008
12. Cardenas-Blanco A, Machts J, Acosta-Cabronero J et al. (2014) Central white matter degeneration in bulbar- and limb-onset amyotrophic lateral sclerosis. J. Neurol. 261(10): 1961–1967
13. Cardenas-Blanco A, Machts J, Acosta-Cabronero J et al. (2016) Structural and diffusion imaging versus clinical assessment to monitor amyotrophic lateral sclerosis. Neuroimage. Clin. 11: 408–414
14. Smith SM, Jenkinson M, Woolrich MW et al. (2004) Advances in functional and structural MR image analysis and implementation as FSL. Neuroimage. 23 Suppl 1: S208-19. doi: 10.1016/j.neuroimage.2004.07.051
15. Fazekas F, Chawluk JB, Alavi A et al. (1987) MR signal abnormalities at 1.5 T in Alzheimer's dementia and normal aging. AJR Am. J. Roentgenol. 149(2): 351–356
16. Smith SM, Jenkinson M, Johansen-Berg H et al. (2006) Tract-based spatial statistics: Voxelwise analysis of multi-subject diffusion data. Neuroimage. 31(4): 1487–1505. doi: 10.1016/j.neuroimage.2006.02.024
17. Avants BB, Epstein CL, Grossman M et al. (2008) Symmetric diffeomorphic image registration with cross-correlation: Evaluating automated labeling of elderly and neurodegenerative brain. Med Image Anal 12(1): 26–41. doi: 10.1016/j.media.2007.06.004
18. Fischl B, Salat DH, Busa E et al. (2002) Whole brain segmentation: automated labeling of neuroanatomical structures in the human brain. Neuron 33(3): 341–355
19. Hyslop NP, White WH (2009) Estimating precision using duplicate measurements. J Air Waste Manag Assoc 59(9): 1032–1039